

Properties of energy-independent nuclear optical potentials

J. T. Londergan

Department of Physics, Indiana University, Bloomington, Indiana 47405

Gerald A. Miller

*Institute for Nuclear Theory and Department of Physics, FM-15,
University of Washington, Seattle, Washington 98195*

(Received 3 August 1981)

For separable, coupled-channel model interactions we show how to construct energy-independent optical potentials, \bar{U} . The elastic phase shifts and nuclear wave functions obtained from \bar{U} are identical at all energies with those of the conventional energy-dependent optical potential $U(E)$. Whenever there is strong absorption or a compound resonance \bar{U} has an extremely rapid variation with momentum.

NUCLEAR REACTIONS Energy-independent optical potentials.
 Separable interaction model; compare momentum dependence of conventional and energy-independent optical potentials; compare with phase-shift-equivalent potentials.

I. INTRODUCTION

It has long been known¹ that in solving the Schrödinger equation describing elastic scattering of a projectile from the ground state of a nuclear target, the inelastic channels describing virtual scattering into the excited states of the target nucleus can be eliminated formally. The resulting one-channel equation contains a nonlocal, complex effective interaction with an explicit dependence on the parametric energy E for the scattering: This effective interaction is the "conventional" optical potential $U(E)$. In practice, $U(E)$ is generally represented by a *local*, but explicitly energy dependent, potential. Many phenomenological studies have been made regarding the energy dependence of $U(E)$ (Refs. 2–5); the theoretical attempts to understand the energy dependence of phenomenological models have led to much insight into nuclear reaction dynamics, as well as to continuing controversy regarding the relation between optical potentials and such concepts as mean free paths of projectiles in nuclei.⁶ Recently, there has been considerable progress in developing microscopic theoretical optical potentials directly from two-nucleon interactions.⁵ All of these methods, however, produce an optical potential which has an explicit dependence upon the parametric energy E .

Recently, Kuo and collaborators derived a new

theory^{7,8} in which the optical potential \bar{U} , although nonlocal, is independent of the energy. However, the potential \bar{U} is constructed in such a way that the elastic scattering phase shifts *and wave functions* obtained from $U(E)$ and \bar{U} are identical at all energies. An energy-independent optical potential, if it can be straightforwardly and accurately calculated, could have many possible uses in nuclear reaction theory. For example, in direct-reaction calculations one could calculate the matrix elements of \bar{U} only once and then use them at all energies. It is even possible that microscopic calculations of the optical potential could be simplified. It is clear that the properties of \bar{U} must be fundamentally different from those of $U(E)$, in order that the two potentials produce the same elastic wave functions at all energies.

For many years physicists have examined "phase-shift-equivalent" potentials.^{9–12} These are two (or more) potentials which are guaranteed to produce the same asymptotic wave function, and hence the same phase shift. As a consequence, the fully on-shell elastic T matrix is identical with two different phase-shift-equivalent potentials. The energy-independent optical potentials of Kuo *et al.* must obey a much more stringent condition, since the construction of \bar{U} requires that the elastic scattering wave function itself (and hence the half off shell elastic T matrix) be identical to the wave

function produced by the conventional optical potential. As a result, we sometimes refer to the potential \bar{U} as a “wave-function-equivalent potential.”

Although some of the properties of the potential \bar{U} have been outlined by Lee *et al.*,⁸ and two different methods have been suggested^{7,8} for constructing a “realistic” energy-independent optical potential \bar{U} , the detailed properties of \bar{U} and the relation between \bar{U} and the conventional optical potential $U(E)$ remain somewhat unclear. As a result, we choose to examine a very simple model—a “two-level” system where the target nucleus has only two possible states, the ground state and one excited state. The interaction potential is given by separable Yamaguchi potentials. We show that such a system has the following features: (i) the elastic scattering wave function can be calculated analytically; (ii) the “conventional” optical potential $U(E)$ can also be calculated analytically; (iii) an integral equation can be obtained for the “energy-independent optical potential” \bar{U} (this integral equation can be straightforwardly solved numerically); (iv) an integral equation can be obtained to produce a phase-shift-equivalent potential which is guaranteed to produce the identical phase shift to our model system.

A brief preliminary report of this work appeared in Ref. 13. The existence of \bar{U} was asserted there, the solution of the integral equation for \bar{U} was presented, and a comparison between the conventional optical potential $U(E)$ and \bar{U} was shown for a single example. In the present paper, we give detailed accounts of the model employed, and the derivation and solution of the integral equation relating $U(E)$ to \bar{U} . To describe the relation between the two potentials, five examples which illustrate various different nuclear reaction phenomena are used. In the context of this model, we find that \bar{U} acquires a very rapid momentum dependence whenever the elastic scattering has either very strong absorption, or a “compound resonance.” Such rapid momentum fluctuations could lead to numerical difficulties in constructing \bar{U} or in evaluating transition matrix elements, if these fluctuations occur in a realistic scattering situation. A final application of these techniques involves pion-nucleon scattering in the P_{33} spin-isospin channel. An energy-independent potential \bar{U} for this system is constructed such that the corresponding on-shell T matrix is a solution of the Low equation.

The outline of this paper is as follows. In Sec. II we derive a general integral equation for \bar{U} . A brief review of the two-level model we are investi-

gating is presented, and the corresponding optical potential $U(E)$ is obtained. The energy-independent optical potential \bar{U} for this model is then constructed. In Sec. III we construct $U(E)$ and \bar{U} for the five different cases under consideration. This allows us to make some general statements about the potential \bar{U} and its momentum dependence. In Sec. IV the techniques of this paper are applied to the pion-nucleon “Chew-Low problem.”¹⁴ An energy-independent effective interaction \bar{U} for pion-nucleon scattering which yields, via the Lippmann-Schwinger equation, a T matrix compatible on shell with the Low equation is obtained. In Sec. V we review a procedure originally introduced by Landau and Tabakin¹¹ for constructing a phase-shift-equivalent (energy independent) separable potential which reproduces the correct elastic scattering phase shift at all energies. A simple relationship between the phase-shift-equivalent potential and \bar{U} is obtained, and the corresponding wave functions are compared. In Sec. VI we summarize our results.

II. ENERGY-DEPENDENT AND ENERGY-INDEPENDENT OPTICAL POTENTIALS

The elastic scattering amplitude $T(E)$, corresponding to nonrelativistic elastic scattering of a projectile from the ground state of a nuclear target, obeys the Lippmann-Schwinger equation

$$T(E) = U(E) + U(E) \frac{1}{E + i\epsilon - H_0} T(E). \quad (2.1)$$

In Eq. (2.1), E is the total projectile-nucleus c.m. energy and H_0 is that part of the total Hamiltonian for the system containing the kinetic energy and the internal Hamiltonian of the target. Feshbach¹ first derived Eq. (2.1) from the original coupled equations which contain the excited states of the target nucleus explicitly. He showed that the effective “optical” potential occurring in Eq. (2.1) is nonlocal and complex (for energies above the first inelastic threshold) and depends on the scattering energy E .

Kuo *et al.*^{7,8} have shown, using folded diagram techniques, that one can *construct* an energy-independent potential \bar{U} which has, at each energy, the same wave function as $U(E)$. If we have an energy-independent potential \bar{U} , then the scattering amplitude $\bar{T}(E)$ corresponding to \bar{U} is given by the integral equation

$$\bar{T}(E) = \bar{U} + \bar{U} \frac{1}{E + i\epsilon - H_0} \bar{T}(E). \quad (2.2)$$

The requirement that \bar{U} and $U(E)$ both produce identical scattering wave functions can be expressed by the momentum-space identity

$$\langle \vec{p} | T(E_k) | \vec{k} \rangle = \langle \vec{p} | \bar{T}(E_k) | \vec{k} \rangle. \quad (2.3)$$

In Eq. (2.3), E_k is the projectile-nucleus energy E corresponding to relative momentum \vec{k} . Equation (2.3), which must be valid for all \vec{p} and \vec{k} , requires that the half-off-shell elastic T matrix elements, and hence the elastic scattering wave functions, be always identical for $U(E)$ and \bar{U} .

We can straightforwardly obtain an integral equation for \bar{U} by explicitly writing the half-off-shell matrix elements of $\bar{T}(E)$,

$$\langle \vec{p} | \bar{T}(E_k) | \vec{k} \rangle = \langle \vec{p} | \bar{U} | \vec{k} \rangle + \int \frac{d\vec{q}}{(2\pi)^3} \langle \vec{p} | \bar{U} | \vec{q} \rangle \frac{1}{E_k - E_q + i\epsilon} \langle \vec{q} | \bar{T}(E_k) | \vec{k} \rangle; \quad (2.4)$$

inserting Eq. (2.3) into (2.4) immediately gives

$$\langle \vec{p} | \bar{U} | \vec{k} \rangle = \langle \vec{p} | T(E_k) | \vec{k} \rangle - \int \frac{d\vec{q}}{(2\pi)^3} \langle \vec{p} | \bar{U} | \vec{q} \rangle \frac{1}{E_k - E_q + i\epsilon} \langle \vec{q} | T(E_k) | \vec{k} \rangle. \quad (2.5)$$

The result, Eq. (2.5), is the desired integral equation for \bar{U} . Given the half-off-shell matrix elements of $T(E)$ as input, (2.5) is a standard matrix equation for the elements of \bar{U} .

By contrast, we present the integral equation relating the matrix elements of the conventional optical potential to the half-off-shell elastic T matrix; this is

$$\langle \vec{p} | U(E_k) | \vec{k} \rangle = \langle \vec{p} | T(E_k) | \vec{k} \rangle - \int \frac{d\vec{q}}{(2\pi)^3} \langle \vec{p} | U(E_k) | \vec{q} \rangle \frac{1}{E_k - E_q + i\epsilon} \langle \vec{q} | T(E_k) | \vec{k} \rangle. \quad (2.6)$$

The optical potential matrix elements which appear on the right-hand side of Eq. (2.6) depend upon the momenta \vec{p} and \vec{q} as well as the parametric energy E_k , whereas the equation for \bar{U} involves only the momenta \vec{p} and \vec{q} .

In order to illustrate the construction of \bar{U} and to compare it with the conventional optical potential $U(E)$, we invoke a very simple model in which the elastic wave functions and $U(E)$ can both be calculated analytically. In this model the projectile interacts via rank-one separable potentials with a nuclear core possessing a bound state and a single internal excitation, with excitation energy Δ . Thus the projectile-nucleus interaction can be written as

$$\langle n' \vec{p} | V | n \vec{k} \rangle \equiv \langle \vec{p} | V_{n'n} | \vec{k} \rangle = \sum_l (2l+1) \lambda^{(l)} v_n^{(l)}(p) v_n^{(l)}(k) P_l(\hat{p} \cdot \hat{k}). \quad (2.7)$$

In Eq. (2.7), $n=0$ ($n=1$) refers to the nuclear ground state (excited state), respectively, e.g., the potential coupling the ground state to the excited state is denoted V_{10} and the diagonal potential for the ground state of the target is V_{00} . The coupling constant $\lambda^{(l)} = \pm 1$ gives the sign of the interaction (attractive or repulsive). Although such a description of nuclear scattering is very specialized and apparently rather limited, it is possible to provide at least a qualitative representation of a large number of nuclear scattering phenomena by a judicious choice of the available parameters.

The elastic scattering amplitude resulting from such a potential has the form

$$\langle \vec{p} | T(E) | \vec{k} \rangle = \sum_l (2l+1) \lambda^{(l)} \frac{v_0^{(l)}(p) v_0^{(l)}(k)}{D^{(l)}(E)} \times P_l(\hat{p} \cdot \hat{k}), \quad (2.8)$$

where

$$D^{(l)}(E) \equiv 1 - \frac{2\lambda^{(l)}}{\pi} \sum_{n=0}^1 \int_0^\infty \frac{q^2 dq [v_n^{(l)}(q)]^2}{E + i\epsilon - E_q^{(n)}}. \quad (2.9)$$

In Eq. (2.9) $E_q^{(n)}$ is the relative c.m. kinetic energy in channel (n) corresponding to momentum q ;

we use nonrelativistic kinematics throughout, so that

$$\begin{aligned} E_q^{(0)} &\equiv \frac{q^2}{2\mu_0}, \\ E_q^{(1)} &\equiv \frac{q^2}{2\mu_1} + \Delta, \end{aligned} \quad (2.10)$$

where

$$\mu_1 \equiv \mu_0 + \Delta.$$

For such a simple system, the conventional optical potential is given by the relation

$$\begin{aligned} \langle \vec{p} | U(E) | \vec{k} \rangle &= \sum_l (2l+1) \lambda^{(l)} \frac{v_0^{(l)}(p) v_0^{(l)}(k)}{D_2^{(l)}(E)} \\ &\quad \times P_l(\hat{p} \cdot \hat{k}), \end{aligned} \quad (2.11)$$

where

$$D_2^{(l)}(E) = 1 - \frac{2\lambda^{(l)}}{\pi} \int_0^\infty dq \frac{q^2 [v_1^{(l)}(q)]^2}{E + i\epsilon - E_q^{(1)}}. \quad (2.12)$$

To obtain the energy-independent optical potential \bar{U} , we assume a solution of the form

$$\begin{aligned} \langle \vec{p} | \bar{U} | \vec{k} \rangle &= \sum_l (2l+1) \lambda^{(l)} v_0^{(l)}(p) \\ &\quad \times \frac{v_0^{(l)}(k)}{\mathcal{D}^{(l)}(k)} P_l(\hat{p} \cdot \hat{k}). \end{aligned} \quad (2.13)$$

Although Eq. (2.13) looks superficially like the equation for the conventional optical potential, we note that $\mathcal{D}^{(l)}(k)$ in Eq. (2.13) is a function of the momentum k , while $D_2^{(l)}(E)$ in Eq. (2.11) is a function of the parametric energy [the differences are also clear by comparing Eqs. (2.5) and (2.6)]. (Note: in subsequent equations wherever possible we work with a single partial wave and suppress all angular momentum indices, to simplify the notation with no loss in generality.)

We can then obtain an integral equation for $\mathcal{D}(k)$ by substituting Eq. (2.13) into the integral equation for \bar{U} , Eq. (2.5). This relation is

$$\begin{aligned} \frac{1}{\mathcal{D}(k)} &= \frac{1}{D(E_k)} - \frac{2}{\pi} \int_0^\infty \frac{dq q^2 \lambda [v_0(q)]^2}{E_k - E_q^{(0)} + i\epsilon} \\ &\quad \times \frac{1}{\mathcal{D}(q) D(E_k)}. \end{aligned} \quad (2.14)$$

The integral equation (2.14) may be converted into an easily solved expression by two steps. First, define

$$F(k) \equiv \frac{D(E_k)}{\mathcal{D}(k)}; \quad (2.15)$$

then make use of the relation between the fully on-shell elastic T -matrix element and the phase shift:

$$\begin{aligned} e^{i\delta(k)} \sin[\delta(k)] &= -2\rho(k) \langle k | T(E_k) | k \rangle \\ &\equiv -2k^2 \frac{dk}{dE_k} \frac{\lambda [v_0(k)]^2}{D(E_k)}. \end{aligned} \quad (2.16)$$

In Eq. (2.16), $\rho(k) \equiv k^2 (dk/dE_k)$ is the density of states, and for the coupled-channel problem the phase shift δ is complex above inelastic threshold. Inserting Eqs. (2.15) and (2.16) into (2.14) gives the integral equation

$$\begin{aligned} F(k) &= 1 + \frac{1}{\pi} \int_{E_{\text{th}}}^\infty \frac{dy}{E_k + i\epsilon - y} \\ &\quad \times e^{i\delta(y)} \sin[\delta(y)] F(y). \end{aligned} \quad (2.17)$$

Equation (2.17) is in a form which has been solved by several previous authors.^{11,15-18} We repeat the derivation in the Appendix, along with the conditions on the phase shift δ necessary for solution of the integral equation. The solution of Eq. (2.17) is

$$\begin{aligned} \frac{1}{\mathcal{D}(k)} &= \left[\frac{E_k + E_B}{E_k} \right] \frac{1}{D(E_k)} \\ &\quad \times \exp \left[\frac{1}{\pi} \int_{E_{\text{th}}}^\infty \frac{dx \delta(x)}{E_k + i\epsilon - x} \right]. \end{aligned} \quad (2.18)$$

In Eq. (2.18), we have assumed that there is a bound state of the projectile-nucleus system with energy $-E_B$ [if there is no bound state, set $E_B = 0$ in Eq. (2.17)]; also, E_{th} is the elastic channel threshold energy.

For our model problem, we can use one further simplification. With the separable potentials we have used, we can show that^{12,18}

$$D(E_k) = \left[\frac{E_k + E_B}{E_k} \right] \exp \left[\frac{1}{\pi} \int_{E_{\text{th}}}^\infty \frac{\hat{\delta}(x) dx}{E_k + i\epsilon - x} \right]. \quad (2.19)$$

In Eq. (2.19), $\hat{\delta}(x)$ is the *real* phase of the T matrix, defined through

$$\{ e^{i\delta(x)} \sin[\delta(x)] \} \\ \equiv | e^{i\delta(x)} \sin\delta(x) | e^{i\hat{\delta}(x)}. \quad (2.20)$$

An explicit formula for $\hat{\delta}$ is given in Ref. 12. The use of (2.19) allows us to obtain a simplified expression for the function $\mathcal{D}(k)$,

$$\frac{1}{\mathcal{D}(k)} = \exp \left[\frac{1}{\pi} \int_{E_{\text{th}}}^{\infty} \frac{dx \{ \delta(x) - \hat{\delta}(x) \}}{E_k + i\epsilon - x} \right]. \quad (2.21)$$

We now have an equation for $\mathcal{D}(k)$ in terms of the elastic channel phase shift δ [knowledge of δ also defines $\hat{\delta}$ via Eq. (2.20)]. For separable, two-channel interactions the conventional optical potential is given by Eq. (2.11), and the *energy-independent* optical potential \bar{U} is given by Eqs. (2.13) and (2.21).

III. SOME NUMERICAL EXAMPLES

In this section, we work out several examples in which $U(E)$ and \bar{U} are constructed and compared. The expressions (2.11), (2.13), and (2.21) are employed.

The potentials we use are rank-one potentials of Yamaguchi form,¹⁹ for $l=0$ or $l=1$, which are defined by

$$v_0^{(l)}(p) = \left[\frac{4\pi a^{3-2l}\alpha}{\mu_0} \right]^{1/2} \frac{p^l}{p^2 + a^2}, \quad (3.1)$$

$$v_1^{(l)}(p) = \left[\frac{4\pi b^{3-2l}\beta}{\mu_1} \right]^{1/2} \frac{p^l}{p^2 + b^2}. \quad (3.2)$$

In Eqs. (3.1) and (3.2), $\{\alpha, \beta\}$ and $\{a, b\}$ are the interaction strengths and ranges for the potential form factors. The masses μ_0 and μ_1 represent the projectile-nucleus mass in the ground and excited states, respectively. If Δ represents the inelastic

channel threshold energy, then we define

$$\mu_1 \equiv \mu_0 + \Delta. \quad (3.3)$$

The parameter λ is always chosen as (-1) , to give an attractive force. By appropriate variation of the ranges and strengths with these potentials, it is possible to simulate a number of different reaction phenomena. The parameters which are used for the five examples for this paper are listed in Table I.

With the Yamaguchi potentials from Eqs. (4.1) and (4.2) we can solve for the elastic wave function and scattering amplitude. With these potentials, $D^{(l)}(E)$ from (2.9) has the form

$$D^{(0)}(E_k) = 1 - \frac{\alpha a^2}{(a - ik)^2} - \frac{\beta b^2}{(b - ik')^2} \quad (3.4)$$

and

$$D^{(1)}(E_k) = 1 + \frac{i\alpha a(2k + ia)}{(a - ik)^2} + \frac{i\beta b(2k' + ib)}{(b - ik')^2}, \quad (3.5)$$

where

$$k' = [2\mu_1 \{ k^2/2\mu_0 - \Delta \}]^{1/2}. \quad (3.6)$$

The potentials have been normalized so that if the channel coupling were set to zero, then the potential would produce a bound state if $\alpha > 1$. The condition for a bound state to be present (these models will produce at most one bound state) are

$$1 - \alpha - \frac{\beta}{\left[1 + \frac{Q}{b} \right]^2} \leq 0 \quad (l=0), \quad (3.7a)$$

$$1 - \alpha - \frac{\beta \left[1 + \frac{2Q}{b} \right]}{\left[1 + \frac{Q}{B} \right]^2} \leq 0 \quad (l=1), \quad (3.7b)$$

TABLE I. Parameters for two-channel separable potential model used to illustrate various reaction mechanisms. The definitions of the symbols are angular momentum l , ranges a and b (MeV), strengths α and β , masses μ_0 and Δ (MeV), and binding energy E_B (MeV) (this is blank if there is no bound state). Parameters as defined in Eqs. (3.1)–(3.3).

Case	l	a (MeV)	α	b (MeV)	β	μ_0 (MeV)	Δ (MeV)	E_B (MeV)
I	1	250	0.87	400	0.30	883	30	12
II	1	250	0.63	400	0.54	883	30	12
III	1	500	0.348	1000	0.578	140	220	
IV	1	250	0.75	400	0.22	883	30	
V	0	250	0.30	400	0.97	883	30	

where

$$Q \equiv [2\mu_1 \Delta]^{1/2}. \quad (3.7c)$$

The bound state energy E_B occurs at a zero of D , i.e., $D^{(l)}(E_B) = 0$. The functions $D_2^{(l)}(E)$, which occur in the expression for the conventional optical potential in this model [see Eq. (2.11)] are obtained from Eqs. (3.4) and (3.5) by setting $\alpha = 0$ in each of these expressions.

For each case considered, we choose the parameters for the model and then calculate analytically the conventional optical potential. Then the elastic phase shifts δ and δ_0 are used to perform the integration in Eq. (2.21) to construct $\mathcal{D}(k)$ and hence

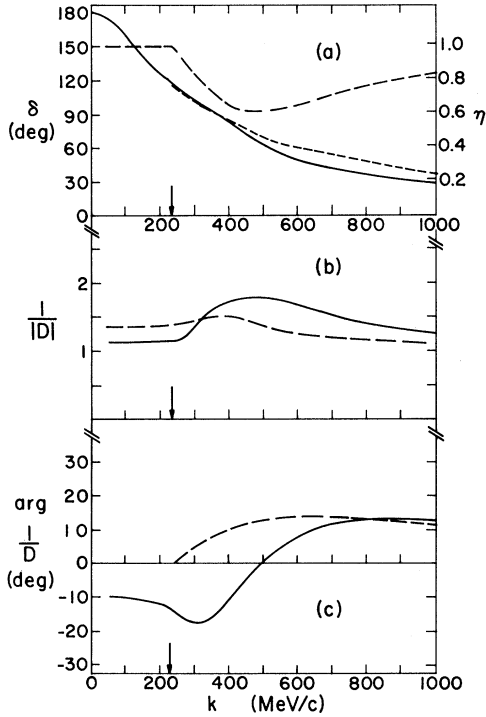


FIG. 1. (a) Phase parameters for case I, “mostly elastic P -wave” case used by HL, Ref. 20. Elastic complex phase shift δ is represented by $\delta = \delta_0 - (i/2) \ln \eta$. Solid curve: δ_0 . Long-dashed curve: η . Short-dashed curve: δ , defined in Eq. (2.20). Phases are plotted vs c.m. momentum k , in MeV/c. The arrow on the horizontal axis denotes the inelastic channel threshold. (b) Magnitude of the functions $[\mathcal{D}(k)]^{-1}$, defined from Eq. (2.21), and $[D_2(E_k)]^{-1}$, defined in Eq. (2.12) vs c.m. momentum k . Solid curve: $|\mathcal{D}(k)|^{-1}$; dashed curve: $|D_2(E_k)|^{-1}$. The functions \mathcal{D} and D_2 allow a direct comparison between the conventional and energy-independent optical potentials, from Eqs. (2.11) and (2.13). (c) Phases of $[\mathcal{D}(k)]^{-1}$, and $[D_2(E_k)]^{-1}$, in degrees, vs c.m. momentum k . Solid curve: $\arg[\mathcal{D}(k)]^{-1}$; dashed curve: $\arg[D_2(E_k)]^{-1}$.

obtain \bar{U} . Since our potentials have the form

$$\langle p | U(E) | k \rangle \sim \frac{v_0(p)v_0(k)}{D_2(E)},$$

$$\langle p | \bar{U} | k \rangle \sim \frac{v_0(p)v_0(k)}{\mathcal{D}(k)},$$

a comparison of $U(E)$ with \bar{U} can be made by comparing the functions $D_2(E)$ and $\mathcal{D}(k)$. The essential difference between the two potentials is that D_2 is a function of the scattering energy E , while \mathcal{D} is a function of the momentum k .

Case I is the “mostly elastic” $l = 1$ case used by Haider and Londergan (HL).²⁰ The projectile is strongly coupled to the ground state of the target, and only weakly coupled to the target excited state. There is a projectile-nucleus bound state at 12 MeV, and the inelastic channel threshold is at 30 MeV. The elastic phase shifts for this case are shown in Fig. 1(a); the phases η and δ_0 are related to the (complex) phase δ by

$$e^{2i\delta} \equiv \eta e^{2i\delta_0}. \quad (3.8)$$

The phases are plotted versus the c.m. momentum k . The arrow in Fig. 1 denotes the momentum

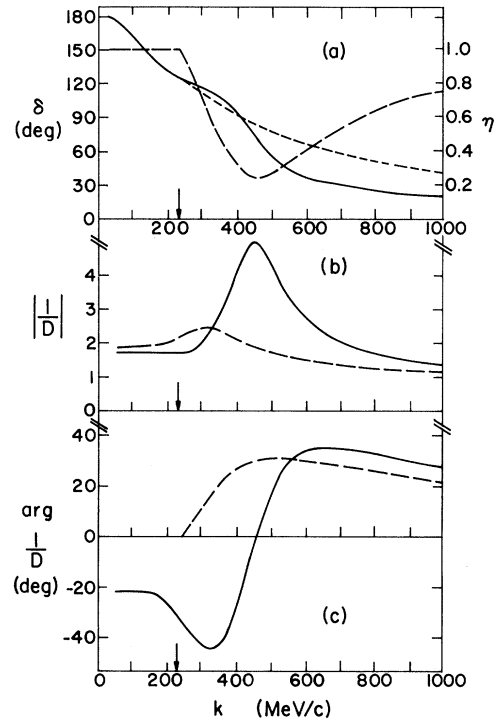


FIG. 2. Phase parameters, $[\mathcal{D}(k)]^{-1}$ and $[D_2(E_k)]^{-1}$ vs c.m. momentum k for case II, “mostly inelastic P -wave” case of HL. Notation is that of Fig. 1.

corresponding to the inelastic channel threshold. Note that below inelastic threshold, $\eta = 1$ and $\hat{\delta} = \delta_0 = \delta$.

In Figs. 1(b) and 1(c), the magnitudes and phases of $[D_2(E_k)]^{-1}$ and $[\mathcal{D}(k)]^{-1}$ are plotted vs c.m. momentum k . For this particular case, both are smooth functions of k . Note that the conventional optical potential is real below inelastic channel threshold, since the imaginary part of $U(E)$ only occurs when there are open inelastic channels, whereas the energy-independent potential \bar{U} (and hence \mathcal{D}) is complex at all momenta.

Case II is the "mostly inelastic" P -wave model of HL. Again there is a bound state at 12 MeV, but the coupling to the inelastic channel is considerably stronger than for case I. As shown in Fig. 2(a), the resulting phases lead to a minimum in η at about 450 MeV/c, where $\eta \sim 0.23$. From Fig. 2(b), we see that $1/\mathcal{D}$ has a prominent maximum at this momentum.

Case III is the very strong absorption P -wave model of Londergan and Moniz.¹⁷ This case was

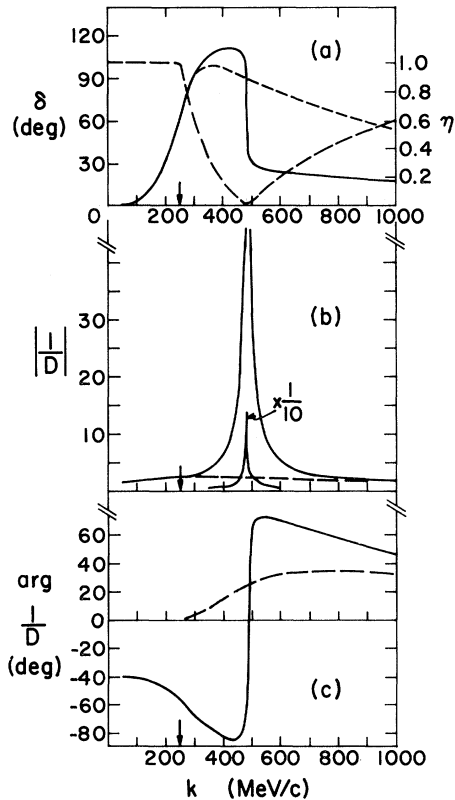


FIG. 3. Phase parameters, $[\mathcal{D}(k)]^{-1}$ and $[D_2(E_k)]^{-1}$ vs c.m. momentum k for case III, "very strong absorption" case used in Refs. 13 and 17. Notation is that of Fig. 1.

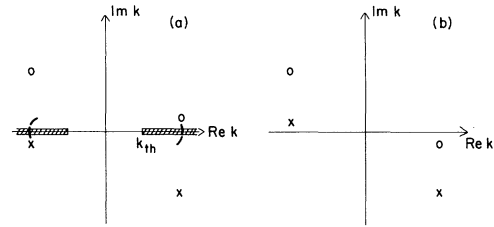


FIG. 4. Schematic diagram of poles and zeroes of the elastic S matrix in the complex k plane (k is the c.m. momentum). Zeroes of S are denoted by 0; poles by \times . (a) The multisheeted k plane with cuts beginning at k_{th} (first inelastic channel threshold). Dashed lines mean that pole or zero is on second sheet of k surface. Poles and zeroes describe situation with a resonance which has more than half its width in inelastic channels, and a zero of S very close to the real axis. (b) The same situation for an "energy-independent" description. In this case there is only a single sheet of the k surface, so that the pole and zero of S which occur on the second sheet of k surface in (a) appear on the first sheet in (b).

discussed briefly in Ref. 13, and is repeated here for completeness. In this case, there is very strong absorption ($\eta \leq 0.01$) for $k \sim 480$ MeV/c as shown in Fig. 3(a). The conventional optical potential for this case varies smoothly with energy; however, $|1/\mathcal{D}|$ has an extremely large maximum which coincides exactly with the minimum in η , and a very rapid change in phase as shown in Figs. 3(b) and (c).

A detailed explanation of this behavior (a very rapid change in \bar{U} associated with a minimum in η) was given in Ref. 12, and we recapitulate it briefly here. Such behavior will occur whenever there is a coupled-channel resonance with more than half its width in inelastic channels. In such a case, a decrease in η exactly coincides with an increase in $|1/\mathcal{D}|$; the smaller η is, the larger $|1/\mathcal{D}|$ will become. In Fig. 4, we show the position of a few of the zeroes (0) and poles (\times) of the S matrix in the complex k plane (k is the elastic channel momentum) for a typical inelastic resonance. The fact that the zero of S in the right-hand k plane is in the lower half plane means that the resonance has an elastic width which is less than half the total resonance width. Since the zero of S shown here is very close to the real axis, then $\eta \sim 0$ at the corresponding value of k .

In Ref. 12 it was shown that the S matrix has the form

$$S(k) = \frac{\mathcal{D}_A(-k)}{\mathcal{D}_A(k)}, \quad (3.9)$$

where

$$\mathcal{D}_A(k) = \left[\frac{E_k + E_B}{E_k} \right] \exp \left[\frac{1}{\pi} \int_{E_{th}}^{\infty} \frac{dy \delta(y)}{E_k + i\epsilon - y} \right]. \quad (3.10)$$

[See Eq. (2.21) and Sec. V.] By construction, $\mathcal{D}_A(k)$ has no zeroes in the upper half plane except for the bound state at energy $-E_B$; similarly, $\mathcal{D}_A(-k)$ has no zeroes in the lower half k plane. The S -matrix zero in the lower half k plane in Fig. 4(b) must therefore come from a pole of $\mathcal{D}_A(k)$. If the zero of $S(k)$ occurs close to the physical region, then $\mathcal{D}_A(k)$ will be extremely large at the corresponding momentum.

Figure 3 (and to a lesser extent Fig. 2) illustrates this behavior. The function $1/\mathcal{D}$ becomes very large just where η , the magnitude of the elastic S -matrix element, becomes smallest. By comparing Eqs. (3.10) and (2.21), we can see that $1/\mathcal{D}(k)$ will become large whenever $\mathcal{D}_A(k)$ is large. The essential difference between the energy-dependent and energy-independent separable potential models is illustrated in Fig. 4. In the *energy-independent* model, the elastic S -matrix element is described in terms of the single-sheeted momentum or k surface. In an energy-dependent approach, the elastic S matrix is described in terms of a multisheeted momentum plane (with an inelastic cut beginning at the first inelastic threshold). The absence of the inelastic cuts in the momentum plane sometimes forces the energy-independent formulation to develop very rapid momentum dependence, as exhibited in Fig. 3. The energy-independent potential \bar{U} acquires a momentum dependence which gives the same elastic wave functions everywhere as $U(E)$. The extremely rapid momentum dependence in this instance would presumably require considerable care both in constructing and evaluating the matrix elements of \bar{U} .

In case III, the coupled-channel resonance had more than half the total width in elastic channels and a consequent very rapid momentum dependence of \bar{U} . If instead we had a coupled-channel resonance with more than half the total width in the elastic channel, the resulting \bar{U} would not have any unusual momentum dependence (an example of such a resonance is seen in the $D_{13} \pi N$ partial wave, as shown in Fig. 4 of Ref. 12).

In cases IV and V, we look at the two different ways in which sharp resonances can occur in the elastic scattering channel. One of these types, illustrated in case IV, we call an elastic resonance.

This is the common resonance situation where the combination of centrifugal repulsion and (essentially elastic) attraction creates a “pocket” which traps the particle and gives rise to a resonance. Such a resonance can obviously be generated with no inelastic channel at all. We choose $l=1$, and the resulting phase shifts are shown in Fig. 5(a); the resonance occurs at $k = 115$ MeV/c. The functions D_2 and \mathcal{D} shown in Figs. 5(b) and (c) are both quite smooth; the energy-independent potential \bar{U} can generate the observed resonance without any unusual momentum dependence.

Case V illustrates what we call the “compound resonance” situation. In this case, the inelastic-channel coupling is sufficiently strong that there would be a bound state in an inelastic channel if it were not coupled to the (lower energy) elastic channel. If the elastic-channel coupling is sufficiently weak, then it is possible to produce a sharp resonance in the elastic channel. This is the standard way in which narrow resonances are produced in low-energy elastic scattering: the conventional optical potential has poles at a given scattering energy, and these poles get converted into narrow elastic-channel resonances.

In the s -wave model which we use, the inelastic channel coupling is almost strong enough to produce a closed-channel bound state ($\beta=0.97$), and

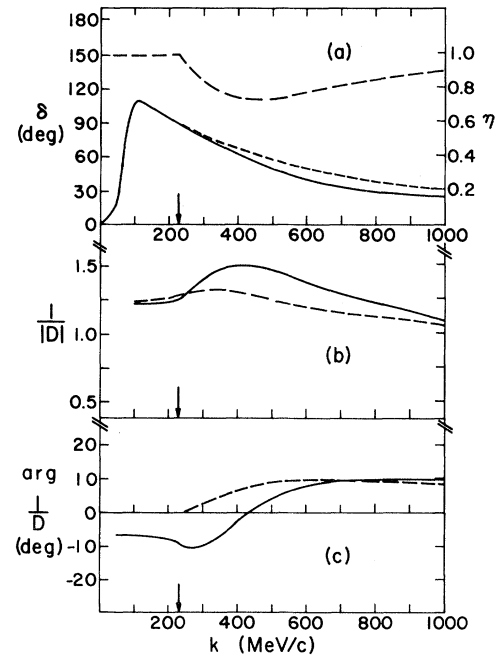


FIG. 5. Phase parameters, $[\mathcal{D}(k)]^{-1}$ and $[D_2(E_k)]^{-1}$ vs c.m. momentum k for model IV, “elastic P -wave resonance.” Notation is that of Fig. 1.

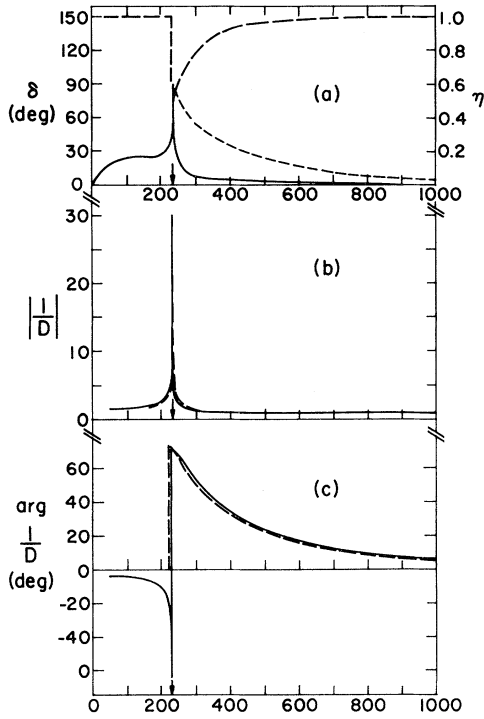


FIG. 6. Phase parameters, $[\mathcal{D}(k)]^{-1}$ and $[D_2(E_k)]^{-1}$ vs c.m. momentum k for case V, "compound $L=0$ resonance." Notation is that of Fig. 1.

the elastic-channel coupling is quite weak. The result is a very sharp resonance which occurs right at the inelastic channel threshold: the phase shift rises very rapidly to 85° and η drops to 0.1, as shown in Fig. 6(a). Both $1/\mathcal{D}$ and $1/D_2$ vary extremely rapidly at threshold, as shown by Figs. 6(b) and (c). We stress the difference between $U(E)$ and \bar{U} here, however. If we construct the scattering amplitude $T(E)$ from the integral equation for $U(E)$, Eq. (2.6), the sharp energy dependence of D_2 can be factored out of the resulting integrals and is relatively easy to handle. However, the extreme momentum dependence of $\mathcal{D}(k)$, and hence \bar{U} , may be more troublesome to handle numerically.

IV. THE CHEW-LOW PROBLEM

In this section we discuss the relevance of the techniques discussed in Sec. II to the Chew-Low (CL) problem.¹⁴ Here the energy dependence of the effective interaction (the analog of the "conventional optical potential" for this problem) arises not from the opening of inelastic channels but from a pole in the T matrix below elastic threshold. The technique of finding wave-function-

equivalent effective interactions (similar to \bar{U} in the previous sections) has been used in finding solutions to the Low equations governing pion-nucleus interactions.^{21,22} If we neglect the crossed pion-nucleon (left-hand) cut in the Low equation, then we show that we can find two different effective interactions, both of which are guaranteed to give the same half-off-shell T matrix at all energies, and one of which is energy independent. We contrast the operator techniques previously used to obtain this result²³ with the methods used in this paper.

If we neglect the left-hand cut term in the pion-nucleon Low equation, then it has been shown²³ that the following operator equation gives an identical T matrix to the CL equation

$$T(E) = \frac{\lambda V_{\text{CL}}}{E} + \frac{\lambda V_{\text{CL}}}{E} \frac{E^2}{h_0^2 (E + i\epsilon - h_0)} T(E). \quad (4.1)$$

The driving term V_{CL} is given by

$$\langle \vec{q} | V_{\text{CL}} | \vec{p} \rangle = \frac{v(q)v(p)}{[2\omega_q 2\omega_p]^{1/2}} 4\pi P(p, q). \quad (4.2)$$

$P(p, q)$ is a spin-isospin projection operator for the resonant (3,3) channel (we suppress spin and isospin labels in this discussion), and ω_q is the energy of the free Hamiltonian h_0 for a pion of momentum q ,

$$\omega_q = (q^2 + m_\pi^2)^{1/2}. \quad (4.3)$$

Here the static model is used because it was employed in the original CL work. The constant λ appearing in Eq. (4.1) is real and negative.

Inserting Eq. (4.2) into (4.1) gives the matrix elements of $T(E)$,

$$\langle \vec{q} | T(E) | \vec{p} \rangle = 4\pi \frac{v(q)v(p)}{[2\omega_q 2\omega_p]^{1/2}} \frac{P(q, p)}{D(E)}, \quad (4.4a)$$

where

$$D(E) = \frac{E}{\lambda} \left[1 - \frac{\lambda E}{\pi} \int_0^\infty \frac{dq q^4 [v(q)]^2}{\omega_q^3 (E + i\epsilon - \omega_q)} \right]. \quad (4.4b)$$

The result (4.4) is just the CL solution neglecting the left hand cut (the function which we call $[D(E)]^{-1}$ is called $h(E)$ by CL) proving that Eq. (4.1) is identical to the T matrix of CL. From Eq.

(4.4b), it is clear that $[D(E)]^{-1}$ has a simple pole at $E=0$ with residue λ . From the relation between $T(E)$ and $D(E)$, it is straightforward to show the relation between the real phase shift δ in the (3.3) channel and the function D .

$$[D(\omega_k)]^{-1} = \frac{-e^{i\delta(\omega_k)} \sin[\delta(\omega_k)]}{[v(k)]^2 k^3}. \quad (4.5)$$

Next, we show that there is an ‘‘optical potential’’ for the CL problem; i.e., an energy-dependent effective interaction $U(E)$ which when inserted into the Lippman-Schwinger integral equation will reproduce the CL T matrix. From Eq. (2.6), the equation which $U(E)$ must satisfy is

$$T(E) = U(E) + U(E) \frac{1}{E + i\epsilon - h_0} T(E). \quad (4.6)$$

The potential $U(E)$ may be obtained directly by equating (4.6) and (4.1); this gives

$$U(E) = \left[E - \lambda V_{\text{CL}}(E + h_0) \frac{1}{h_0} \right]^{-1} \lambda V_{\text{CL}}. \quad (4.7)$$

The optical potential $U(E)$ has an explicit energy dependence. We next find an energy-independent potential \bar{V} which produces the same half-off-shell matrix elements as $U(E)$. First the operator approach of Ref. 23 is used. Define the operator $\mathcal{S}(E)$ by

$$\mathcal{S}(E) = T(E) E \frac{1}{h_0}. \quad (4.8)$$

By inspection, the half-off-shell matrix elements of $\mathcal{S}(E)$ and $T(E)$ are identical

$$\langle \vec{p} | \mathcal{S}(\omega_k) | \vec{k} \rangle = \langle \vec{p} | T(\omega_k) | \vec{k} \rangle. \quad (4.9)$$

From Eq. (4.1), we see that $\mathcal{S}(E)$ obeys the integral equation

$$\mathcal{S}(E) = \lambda V_{\text{CL}} \frac{1}{h_0} \left[1 + E \frac{1}{h_0} \frac{1}{E + i\epsilon - h_0} \mathcal{S}(E) \right]. \quad (4.10)$$

The energy-independent potential \bar{V} must satisfy the integral equation

$$\mathcal{S}(E) = \bar{V} + \bar{V} \frac{1}{E + i\epsilon - h_0} \mathcal{S}(E). \quad (4.11)$$

We can obtain \bar{V} by equating (4.11) and (4.10); this gives the integral equation

$$\bar{V} = \lambda V_{\text{CL}} \frac{1}{h_0} \left[1 + \frac{1}{h_0} \bar{V} \right]. \quad (4.12)$$

Clearly, \bar{V} in Eq. (4.12) is independent of energy. An explicit form for \bar{V} is obtained by substituting V_{CL} from Eq. (4.2) into (4.12)

$$\langle \vec{q} | \bar{V} | \vec{p} \rangle = \frac{4\pi v(q)v(p)}{[2\omega_q 2\omega_p]^{1/2}} \frac{P(q,p)}{\omega_p} \frac{\lambda}{1-\alpha}, \quad (4.13)$$

where

$$\alpha \equiv \frac{\lambda}{\pi} \int_0^\infty \frac{dq [qv(q)]^2}{\omega_q^3}. \quad (4.14)$$

Direct substitution of (4.13) into (4.11) shows that Eq. (4.9) is correct.

Next, we obtain an energy-independent optical potential \bar{V} for the CL problem applying the methods of Sec. II of this paper. First, note that Eqs. (4.4b) and (4.5) can be rewritten as

$$\frac{\lambda D(E)}{E} = 1 - \alpha + \frac{1}{\pi} \int_{m_\pi}^\infty dy \frac{e^{i\delta(y)} \sin[\delta(y)]}{E + i\epsilon - y} \times \frac{\lambda D(y)}{y}. \quad (4.15)$$

Now define

$$f(z) \equiv \frac{\lambda D(z)}{(1-\alpha)z}, \quad (4.16)$$

so that Eq. (4.15) can be simplified:

$$f(z) = 1 + \frac{1}{\pi} \int_{m_\pi}^\infty dy \frac{e^{i\delta(y)} \sin[\delta(y)]}{z - y} f(y). \quad (4.17)$$

Equation (4.17) is identical to Eq. (A4) of the Appendix; following the steps outlined there, one can write immediately

$$\frac{\lambda D(E_k)}{E_k} = (1-\alpha) \exp \left[\frac{1}{\pi} \int_{m_\pi}^\infty \frac{dy \delta(y)}{E_k + i\epsilon - y} \right]. \quad (4.18)$$

Next, following the logic of Sec. II and Eq. (4.2), we assume a form for \bar{U} ,

$$\langle \vec{p} | \bar{U} | \vec{k} \rangle = \frac{4\pi v(p)v(k)}{[2\omega_p 2\omega_k]^{1/2}} \frac{\lambda P(p,k)}{\mathcal{D}(\omega_k)}. \quad (4.19)$$

Inserting (4.19) into (4.11) and making use of (4.5) gives

$$\frac{D(\omega_k)}{\mathcal{D}(\omega_k)} = 1 + \frac{1}{\pi} \int_{m_\pi}^{\infty} \frac{dy e^{i\delta(y)} \sin \delta(y)}{\omega_k + i\epsilon - y} \left\{ \frac{D(y)}{\mathcal{D}(y)} \right\}. \quad (4.20)$$

Equation (4.20) is identical with Eq. (4.17) if a quantity

$$f(z) \equiv \frac{D(z)}{\mathcal{D}(z)}, \quad (4.21)$$

is defined.

Both (4.16) and (4.21) satisfy identical integral equations with identical boundary values, so that one can equate the two solutions for physical energies; this gives

$$\frac{1}{\mathcal{D}(\omega_k)} = \frac{1}{\omega_k(1-\alpha)}. \quad (4.22)$$

Substituting this into Eq. (4.19) yields the result that the solution \bar{U} in Eq. (4.19) is identical to the potential \bar{V} of Eq. (4.13), defined via the operator methods of Ref. 23.

V. COMPARISON OF WAVE-FUNCTION-EQUIVALENT AND CERTAIN PHASE-SHIFT-EQUIVALENT POTENTIALS

In this section the elastic channel wave functions obtained from $U(E)$ are compared with those of another model, Ref. 11. In that work an energy-independent potential, V_A is obtained. Although V_A and $U(E)$ have the same phase shifts, the corresponding wave functions are different.

We begin by using $U(E)$ [(2.11) and (2.12)] to obtain the elastic channel wave function in the momentum representation,

$$\langle \vec{p} | \psi(E_k) \rangle = (2\pi)^3 \delta(\vec{p} - \vec{k}) + \sum_l \frac{\lambda^{(l)} v_0^{(l)}(p) v_0^{(l)}(k) (2l+1) P_l(\hat{p} \cdot \hat{k})}{[E_k - E_p + i\epsilon] D^{(l)}(E_k)}. \quad (5.1)$$

In Eq. (5.1), $|\psi(E_k)\rangle$ is the elastic wave function corresponding to c.m. energy E_k (or c.m. momentum k). The Jost function $D^{(l)}(E_k)$ appearing in Eq. (5.1) is given by Eq. (2.19), which is repeated for clarity,

$$D^{(l)}(E_k) = \left[\frac{E_k + E_B}{E_k} \right] \exp \left[\frac{1}{\pi} \int_{E_{th}}^{\infty} \frac{\hat{\delta}^{(l)}(y) dy}{E_k - i\epsilon - y} \right]. \quad (5.2)$$

Here $(-E_B)$ is the energy of the bound state in the l th partial wave for the system ($E_B = 0$ if there is no bound state), and $\hat{\delta}^{(l)}(E)$ is the real phase of the elastic T matrix at energy E . We can define the on-shell T -matrix element $t_l(E_k)$ as

$$\langle \vec{k} | T^{(l)}(E_k) | \vec{k} \rangle = \frac{\lambda^{(l)} (2l+1) [v_0^{(l)}(k)]^2}{D^{(l)}(E_k)} \equiv t_l(E_k), \quad (5.3)$$

and rewrite the elastic wave function as

$$\langle \vec{p} | \psi(E_k) \rangle = (2\pi)^3 \delta(\vec{p} - \vec{k}) + \sum_l \left\{ \frac{v_0^{(l)}(p)}{v_0^{(l)}(k)} \right\} \frac{1}{E_k - E_p + i\epsilon} \times t_l(E_k) P_l(\hat{p} \cdot \hat{k}). \quad (5.4)$$

The potential \bar{U} defined in Sec. II is guaranteed to produce exactly the same elastic wave function as Eq. (5.4) at all energies; for this reason we call \bar{U} a wave-function-equivalent potential. Since the elastic wave function can be exactly calculated in this model, it is instructive to compare the optical potential \bar{U} with a phase-shift-equivalent potential, which reproduces the *asymptotic form* of the elastic wave function (i.e., the phase shift or the fully-on-shell T matrix) at all energies, but will not give the exact wave function. We do this for two reasons. First, there exist methods for constructing phase-shift-equivalent absorptive separable potentials (ASP).¹¹ These techniques can be used to construct an elastic channel wave function which has the same phase shift everywhere as our model wave function. It is instructive to compare this wave function to our exact result. Second, a simple relationship between the absorptive separable potential and our energy-independent potential \bar{U} can be obtained.

The absorptive (energy-independent) separable potential approach was developed by Landau and Tabakin (LT) (Ref. 11) and applied to π - N potentials. If the elastic phase shift in the l th partial wave $\delta^{(l)}$ is known at all energies, LT showed that a separable potential V_A could be constructed which was guaranteed to exactly reproduce $\delta^{(l)}$ everywhere. The "absorptive separable potential" V_A has the momentum representation

$$\langle \vec{p} | V_A | \vec{q} \rangle = \sum_l \lambda^{(l)} (2l+1) v_A^{(l)}(p) \times v_A^{(l)}(q) P_l(\hat{p} \cdot \hat{q}). \quad (5.5)$$

The form factors v_A occurring in Eq. (5.5) are defined by

$$\lambda^{(l)}[v_A(k)]^2(2l+1) = \langle \vec{k} | T^{(l)}(E_k) | \vec{k} \rangle \mathcal{D}_A^{(l)}(E_k), \quad (5.6)$$

where

$$\mathcal{D}_A^{(l)}(E_k) = \left[\frac{E_k + E_B}{E_k} \right] \exp \left[\frac{1}{\pi} \int_{E_{th}}^{\infty} \frac{\delta^{(l)}(y) dy}{E_k + i\epsilon - y} \right]. \quad (5.7)$$

With the separable potential of Eq. (5.5), one can immediately write the corresponding elastic wave function $|\psi_A\rangle$ in momentum space,

$$\begin{aligned} \langle \vec{p} | \psi_A(E_k) \rangle &= (2\pi)^3 \delta(\vec{p} - \vec{k}) \\ &+ \sum_l \frac{\lambda^{(l)} v_A^{(l)}(p) v_A^{(l)}(k)}{[E_k - E_p + i\epsilon]} \\ &\times (2l+1) P_l(\hat{p} \cdot \hat{k}), \end{aligned} \quad (5.8)$$

or alternatively

$$\begin{aligned} \langle \vec{p} | \psi_A(E_k) \rangle &= (2\pi)^3 \delta(\vec{p} - \vec{k}) \\ &+ \sum_l \left\{ \frac{v_A^{(l)}(p)}{v_A^{(l)}(k)} \right\} \frac{1}{E_k - E_p + i\epsilon} \\ &\times t_l(E_k) P_l(\hat{p} \cdot \hat{k}). \end{aligned} \quad (5.9)$$

Compare the exact model wave function $|\psi\rangle$ of Eq. (5.4) with the phase-shift-equivalent wave function $|\psi_A\rangle$ of Eq. (5.9), and observe that although $|\psi_A\rangle$ has the correct phase shift, the momentum components of $|\psi_A\rangle$ are clearly different from those of the exact wave function.

Next, we compare our energy-independent potential \bar{U} with the phase-shift-equivalent potential V_A . Recall from Eqs. (2.13) and (2.21) that \bar{U} has the form

$$\langle \vec{p} | \bar{U} | \vec{k} \rangle = \sum_l \frac{\lambda^{(l)} v_0^{(l)}(p) v_0^{(l)}(k)}{\mathcal{D}^{(l)}(E_k)} P_l(\hat{p} \cdot \hat{k}), \quad (5.10)$$

where

$$\mathcal{D}^{(l)}(E) = \exp \left[\frac{1}{\pi} \int_{E_{th}}^{\infty} \frac{dy \{ \hat{\delta}(y) - \delta(y) \}}{E + i\epsilon - y} \right]. \quad (5.11)$$

It is not obvious that there should be any simple relation between \bar{U} and V_A , since V_A reproduces the phase shift everywhere but not the elastic wave

function, and \bar{U} correctly reproduces the elastic wave function (and hence the half-off-shell T matrix) at all energies. However, by comparing Eq. (5.11) with (5.7) and (5.2) one finds that

$$\mathcal{D}(E_k) = \frac{D(E_k)}{\mathcal{D}_A(E_k)} = \left[\frac{v_0(k)}{v_A(k)} \right]^2 \quad (5.12)$$

(angular momentum indices are suppressed for the sake of clarity). Consequently, we can write the energy-independent potential \bar{U} in terms of the elastic and absorptive potential form factors,

$$\begin{aligned} \langle \vec{p} | \bar{U} | \vec{k} \rangle &= \sum_l \lambda^{(l)} v_0^{(l)}(p) \frac{[v_A^{(l)}(k)]^2}{v_0^{(l)}(k)} \\ &\times (2l+1) P_l(\hat{p} \cdot \hat{k}). \end{aligned} \quad (5.13)$$

In the simple model which we employ, the conventional optical potential is a separable potential with form factor $v_0(p)$ with a coupling constant (or potential strength) which depends explicitly upon the energy E . We can also construct an absorptive separable potential V_A which reproduces the elastic phase shift at all energies. An energy-independent optical potential \bar{U} can be obtained which produces the exact elastic scattering wave function at all energies. Somewhat surprisingly, in this particular model one can write the matrix elements of \bar{U} in terms of the form factors v_A and v_0 ; consequently, knowledge of the properties of v_A can be used to infer the properties of \bar{U} (see the discussions in Refs. 12 and 18).

VI. SUMMARY

It is very appealing to consider the possibility of constructing energy-independent potentials at all energies. Such potentials suggest a great savings in time and complexity for use in nuclear reaction analysis. Although some of the general properties of these wave-function-equivalent potentials \bar{U} have been enumerated by Kuo *et al.*,^{7,8} it is unclear whether \bar{U} must develop unusual momentum dependence, poles, etc., in order to accommodate all of the scattering, resonance, and bound state phenomena in one energy-independent form.

In order to examine some of these questions, we use a very specific model—that of a projectile interacting via rank-one separable potentials with a target which has only two states (the “ground state” and one “excited state”). Although this restriction is quite severe, it does have many appeal-

ing features. First, we can solve exactly for the elastic scattering wave functions and the conventional optical potential with such a model. There is sufficient flexibility with this model so that a number of different nuclear reaction phenomena—elastic resonances, “compound resonance,” strong absorption, etc., can be reproduced. We can also construct and analyze the energy-independent potential \bar{U} . It is found that \bar{U} develops very rapid momentum dependence under two general conditions: first, whenever there is very strong absorption in a given partial wave, and second, whenever a narrow “compound resonance” occurs in a given partial wave.

In our model, poles or zeroes of the S matrix which occur “naturally” in a multichannel (or energy-dependent) description of the process can lead to very rapid behavior of the energy-independent \bar{U} . Although we cannot extend our methods to a *general* energy-independent potential, our results suggest that some care be taken in constructing energy-independent potentials for systems of particles which have either narrow compound resonances or strongly inelastic resonances.

One may also compare a phase-shift-equivalent potential (the ASP method for constructing phase-shift-equivalent separable potentials given the elastic phase shift at all energies) with our exact model and with the wave-function-equivalent potential \bar{U} . In our separable model, there is a simple relation, (5.13), between \bar{U} and the ASP form factors.

The Chew-Low (CL) problem¹⁴ may be analyzing using our techniques. Previously, it has been demonstrated²³ that an energy-independent potential can be constructed which exactly reproduces the half-off shell T matrix. It is shown that the methods employed in this paper to construct the energy-independent potential \bar{U} can also be used for the CL problem.

This research was supported in part by the U. S. Department of Energy and the National Science Foundation.

APPENDIX: SOLUTION OF THE INTEGRAL EQUATION FOR \bar{U}

In Sec. II of the text, we assume a form for the energy-independent optical potential in our separable-potential model

$$\langle p | \bar{U} | k \rangle = \frac{v_0(p)v_0(k)}{\mathcal{D}(k)} ; \quad (\text{A1})$$

from the integral equation for \bar{U} in terms of the half-off-shell elastic T matrix, Eq. (2.5), we obtain the following integral equation [Eq. (2.17)],

$$F(k) = 1 + \frac{1}{\pi} \int_{E_{\text{th}}}^{\infty} \frac{dy}{E_k + i\epsilon - y} e^{i\delta(y)} \times \sin[\delta(y)] F(y) . \quad (\text{A2})$$

In Eq. (A2), δ is the elastic scattering phase shift, which is complex above inelastic threshold energy, E_{th} is the threshold energy for the elastic channel, and

$$F(k) \equiv \frac{D(E_k)}{\mathcal{D}(k)} , \quad (\text{A3})$$

where $D(E)$ is given by Eqs. (2.8) and (2.9).

Integral equations of the form (A2) have been solved for constructing phase-shift-equivalent separable potentials. We review here the method of solving this equation. Define a function $f(z)$ for complex variable z by the relation

$$f(z) \equiv 1 + \frac{1}{\pi} \int_{E_{\text{th}}}^{\infty} \frac{dy e^{i\delta(y)} \sin[\delta(y)]}{z - y} F(y) ; \quad (\text{A4})$$

note that f is related to F via

$$F(k) = \lim_{\epsilon \rightarrow 0^+} f(z = E_k + i\epsilon) . \quad (\text{A5})$$

The function $f(z)$ is analytic in the cut z plane, with a branch cut along the real z axis beginning at $z = E_{\text{th}}$. From Eq. (A4) one can show that the discontinuity of $f(z)$ across the branch cut is

$$\frac{f(x + i\epsilon) - f(x - i\epsilon)}{2i\epsilon} = e^{-2i\delta(x)} , \quad (x > E_{\text{th}}) . \quad (\text{A6})$$

It is useful to define a function $L(z)$ by

$$L(z) = \ln f(z) , \quad (\text{A7})$$

with discontinuity

$$L(x + i\epsilon) - L(x - i\epsilon) = -2i\delta(x) , \quad (x > E_{\text{th}}) . \quad (\text{A8})$$

Equation (A4) relates $f(z)$ to an integral containing the S -matrix element (in the form of the phase shift δ). If there are no bound states, and if the S matrix is not zero for any scattering energy, then $L(z)$ as defined from Eqs. (A7) and (A8) is analytic in the first sheet of the cut z plane. In this case, one has

$$L(z) = \frac{1}{2\pi i} \oint_C \frac{dy L(y)}{y - z} , \quad (\text{A9})$$

where the contour C is shown in Fig. 7(a). Provided the phase shift δ goes to zero as $E \rightarrow \infty$, we can rewrite Eq. (A9) as

$$L(z) = \frac{1}{\pi} \int_{E_{\text{th}}}^{\infty} \frac{dy \delta(y)}{z-y}, \quad (\text{A10})$$

which leads immediately to the expression

$$\frac{1}{\mathcal{D}(k)} = \frac{1}{D(E_k)} \exp \left[\frac{1}{\pi} \int_{E_{\text{th}}}^{\infty} \frac{\delta(y) dy}{E_k + i\epsilon - y} \right]. \quad (\text{A11})$$

If there is a bound state at $E = -E_B$, then the S matrix has a pole at $E = -E_B$, and $L(z)$ has a logarithmic singularity there. In that case, there is an additional branch cut for the function $L(z)$ along the real axis from $-E_B$ to E_{th} ; Eq. (A9) is still valid, but the contour C must be changed to that shown in Fig. 7(b). Evaluation of the necessary integrals then gives

$$L(z) = \ln \left[\frac{z + E_B}{z} \right] + \frac{1}{\pi} \int_{E_{\text{th}}}^{\infty} \frac{dy \delta(y)}{z-y}, \quad (\text{A12})$$

and the resulting expression for $D(k)$ is

$$\frac{1}{\mathcal{D}(k)} = \left[\frac{E_k + E_B}{E_k} \right] \frac{1}{D(E_k)} \times \exp \left[\frac{1}{\pi} \int_{E_{\text{th}}}^{\infty} \frac{dy \delta(y)}{E_k + i\epsilon - y} \right]. \quad (\text{A13})$$

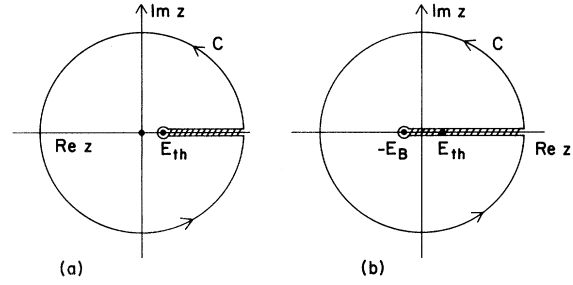


FIG. 7. Integration contours for the function $L(z)$ defined in Eq. (A7). (a) Case where there is no bound state. Then $L(z)$ is analytic in the z plane cut along the real axis from E_{th} to ∞ (z is the analytic continuation of the elastic scattering energy). (b) The situation when there is a bound state at energy $-E_B$. Then, in addition to the cut from E_{th} to ∞ , $L(z)$ has an additional branch cut from $-E_B$ to E_{th} , since $L(z)$ has a logarithmic singularity at $z = -E_B$.

This is Eq. (2.18) in the text. Note that Eq. (A13) reduces to (A11) if we set $E_B = 0$; so if there is no bound state, we simply set $E_B = 0$ in Eq. (A13).

The requirements on the phase shift δ in order that $\mathcal{D}(k)$ be defined from Eq. (A13) are

(i) $\delta(E) \rightarrow 0$ as $E \rightarrow \infty$.

(ii) $\delta(E_{\text{th}})$ equals 0 if there is no bound state, and equals π if there is a bound state (this procedure fails if the system has more than one bound state).

(iii) $S(E) \equiv e^{2i\delta(E)}$ is never zero, for real E .

(iv) $\sin[\delta(E)]$ does not change sign below the inelastic channel threshold.

¹H. Feshbach, Ann. Phys. (N.Y.) 5, 357 (1958); 19, 287 (1962).

²A. Bohr and B. R. Mottelson, *Nuclear Structure* (Benjamin, New York, 1969), Vol. I, p. 237.

³P. E. Hodgson, *Nuclear Reactions and Nuclear Structure* (Clarendon, Oxford, 1971).

⁴A. K. Kerman, H. McManus, and R. M. Thaler, Ann. Phys. (N.Y.) 8, 551 (1959).

⁵*Microscopic Optical Potentials*, Lecture Notes in Physics No. 89, edited by H. V. von Geramb (Springer, New York, 1979).

⁶R. M. DeVries and J. C. Peng, Phys. Rev. Lett. 43, 1373 (1980).

⁷T. T. S. Kuo, F. Osterfeld, and S. Y. Lee, Phys. Rev. Lett. 45, 786 (1980).

⁸S. Y. Lee, F. Osterfeld, K. Tam, and T. T. S. Kuo, Phys. Rev. C 24, 329 (1981).

⁹P. U. Sauer, Phys. Rev. Lett. 32, 626 (1974); D. D.

Brayshaw, Phys. Rev. Lett. 32, 382 (1974).

¹⁰N. J. McGurk, H. de Groot, H. Fiedeldey, and H. J. Boersma, Phys. Lett. 49B, 13 (1974).

¹¹R. Landau and F. Tabakin, Phys. Rev. D 5, 2746 (1972).

¹²J. T. Londergan, K. W. McVoy, and E. J. Moniz, Ann. Phys. (N.Y.) 86, 147 (1974).

¹³J. T. Londergan and G. A. Miller, Phys. Rev. Lett. 46, 1545 (1981).

¹⁴G. F. Chew and F. E. Low, Phys. Rev. 101, 1570, 1579 (1956).

¹⁵M. Goldberger and K. M. Watson, *Collision Theory* (Wiley, New York, 1964), Appendix G. 2.

¹⁶R. Omnes, Nuovo Cimento 8, 316 (1958).

¹⁷J. T. Londergan and E. J. Moniz, Phys. Lett. 45B, 195 (1973).

¹⁸D. J. Ernst, J. T. Londergan, E. J. Moniz, and R. M. Thaler, Phys. Rev. C 10, 1708 (1974).

¹⁹Y. Yamaguchi, Phys. Rev. 95, 1628 (1954).

²⁰Q. Haider and J. T. Londergan, Phys. Rev. C 23, 19 (1981).

²¹G. A. Miller, Phys. Rev. C 16, 2325 (1977).

²²M. A. Alberg, E. M. Henley, G. A. Miller, and J. F.

Walker, Nucl. Phys. A306, 441 (1978); C. Y. Cheung, E. M. Henley, and G. A. Miller, *ibid.* A305, 342 (1978).

²³G. A. Miller, Phys. Rev. C 14, 2230 (1976).